Electronic supplementary materials *Mendeleev Commun.*, 2027, **37**, just accepted

Lithium anode surface modified by *in situ* polymerization of oligomers with diacrylate groups

Alena V. Yudina, Anna A. Slesarenko, Galiya Z. Tulibaeva, Evgeny N. Kabachkov, Yuriy I. Baluda, Alexander V. Mumyatov and OlgaV. Yarmolenko

Table of Contents

Experimental section S2

Figure S1. Structures of the PEGDA: (a) initial structure, (b) stitched branched structure S3

Table S1. Composition of electrolytes S3

Figure S2. Nyquist plots of Li/LE/PI cells during lithiation (a) /delithiation (b) S4

Figure S3. Nyquist plots Li//PI cells with electrolytes: (a-b) LE + 5% Pol-1, (c-d) LE + 10% Pol-1; (i-f) LE + 5% Pol-2, (g-h) LE + 10% Pol-2 during lithiation (a,c,i,g) /delithiation (b,d,f,h) S4-S5

Figure S4. Equivalent circuit of Li//PI cell, where R1 – electrolyte resistance, R2 – charge-transfer resistance at the lithium/electrode interface, CPE – constant phase element S5

Table S2. Calculation of the parameters of the equivalent circuit of the Li/PI cell S5

Figure S5. Optical images of the lithium anode surface S6

Figure S6. FTIR spectra, where ***1:*** lithium surface after testing in a cell with a liquid electrolyte, ***2***: lithium surface after testing in a cell with a oligomer-containing electrolyte S6

Table S3. Assignment of characteristic peaks of SEI S7

Scheme S1. The diglyme decomposition reaction S7

Scheme S2. The LiTFSI decomposition reactions S7

Experimental section

To prepare the solutions of electrolyte, we used the salt $LiN(SO_2CF_3)_2$, lithium bis(trifluoromethanesulfonyl)imide (LiTFSI, purity 99%, commercial product, Sigma Aldrich), and bis(2-methoxyethyl) ether (diglyme, G2, purity ≥99%, Sigma Aldrich) as a solvent. Electrolytes were prepared in an MBraun argon glove box; the samples were weighed on an analytical balance with an accuracy of 0.0001 g.

Polyethylene glycol diacrylate (PEGDA, Aldrich, M_n = 575, T_{melt} = –10 °C; T_g = –73.5 °C) and (PEGDA, Aldrich, M_n = 700, T_{melt} = 12–17 °C) were used as additives in the electrolyte [Figure S1(*a*)**].** Polymerization occurs when C=C bonds are opened by an electric current [Figure S1(*b*)**].**

(*a*)

(*b*)

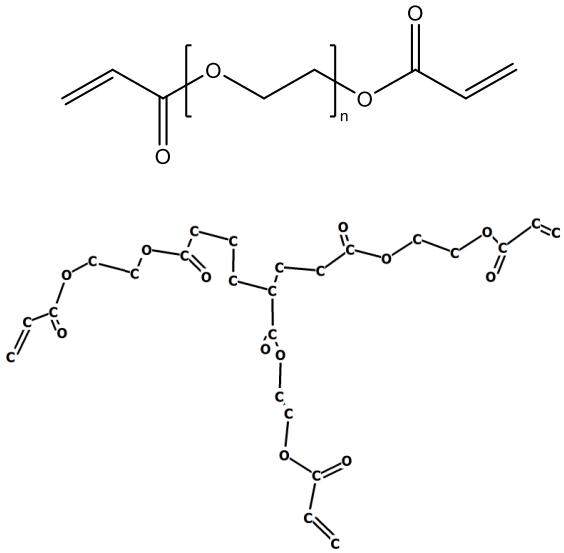


Figure S1 Structures of the PEGDA: (*a*) initial structure, (*b*) stitched branched structure.

Li-Battery Fabrication

The electrochemical performance of polyimide was evaluated in the CR2032 coin-type lithium batteries. The cathode composition comprising of polyimide (45 wt%), conductive carbon black (45 wt%, Timical Super C65), SiO_2 nanoparticles (5 wt%, average particle size 7 nm, Aerosil 380) and PVDF polymer binder (5 wt%, Kynarflex HSV 900, Arkema France) was dispersed in *N*-methylpyrrolidone (NMP, 99%, Aldrich) to obtain ~12% suspension, which was homogenized mechanically. Cathode slurry was applied onto the current collector (20 μm thick graphitized Al-foil, MTI Corp., USA) using tape coating (Gelon Lib. coater). The resulting cathode films were annealed at 160 °C, pressed on rollers and dried again for 5 h at the temperature of 120 °C to remove the NMP solvent. The cathode material loading is 1.2 mg cm^{-2} on the polyimide and 3 mg cm^{-2} on the complete cathode (on the current collector surface).

The organic cathode (d = 1.6 cm), fiber glass separator (Whatman GF/A Glass microfiber filters, GE Healthcare, Chicago, IL, USA), and lithium anode (d = 1.6 cm) were assembled in coin-type lithium batteries using ~30 mkl electrolyte (1 M LiTFSI in G2). The cells were assembled inside MBraun argon glove box.

Li-Battery Testing

Cyclic voltammograms in Li//PI cells were recorded on a P-40X potentiostat (Elins, Russia) at a sweep rate of 2 mV s^{-1}.

The electrochemical characteristics of the cells were evaluated using a BTS-5V10mA battery analyzer (Neware Technology Ltd., China) cycling at different current values in the range of 1.5–3.5 V. The Li/Pi cells were tested at room temperature and at 100 °C at a current density of 40 mA g^{-1}. The calculation of the discharge capacity was carried out on the active mass of the cathode. Cathode capacity (per unit area) ≈ 0.192 mAh cm^{-2}, Li deposition depth (with a 10-fold excess of lithium relative to the cathode) ≈ 1.92 mAh cm^{-2}, Li layer thickness ≈ 0.93 μm.

Research methods

XPS spectra were obtained using a Specs PHOIBOS 150 MCD9 electronic spectrometer (Specs, Berlin, Germany), equipped with a magnesium anode (Mg *Kα* radiation is 1253.6 eV). When recording spectra, the vacuum in the spectrometer chamber did not exceed 3 × 10^{-10} Torr, and the source power was 150 W. The spectra were recorded in the constant transmission energy mode (40 eV for the survey spectra and 10 eV for individual lines). The survey spectra were recorded with a step of 1 eV, and the high-resolution spectra of individual lines – with a step of 0.1 eV.

Table S1 Composition of electrolytes.

No.	Abbreviation	Composition of liquid electrolyte
1	LE	1 M LiTFSI in diglyme (G2)
2	LE + 5 % Pol-1	1 M LiTFSI in G2 + 5 wt% PEGDA-575
3	LE + 10 % Pol-1	1 M LiTFSI in G2 + 10 wt% PEGDA-575
4	LE + 5 % Pol-2	1 M LiTFSI in G2 + 5 wt% PEGDA-700
5	LE + 10 % Pol-2	1 M LiTFSI in G2 + 10 wt% PEGDA-700

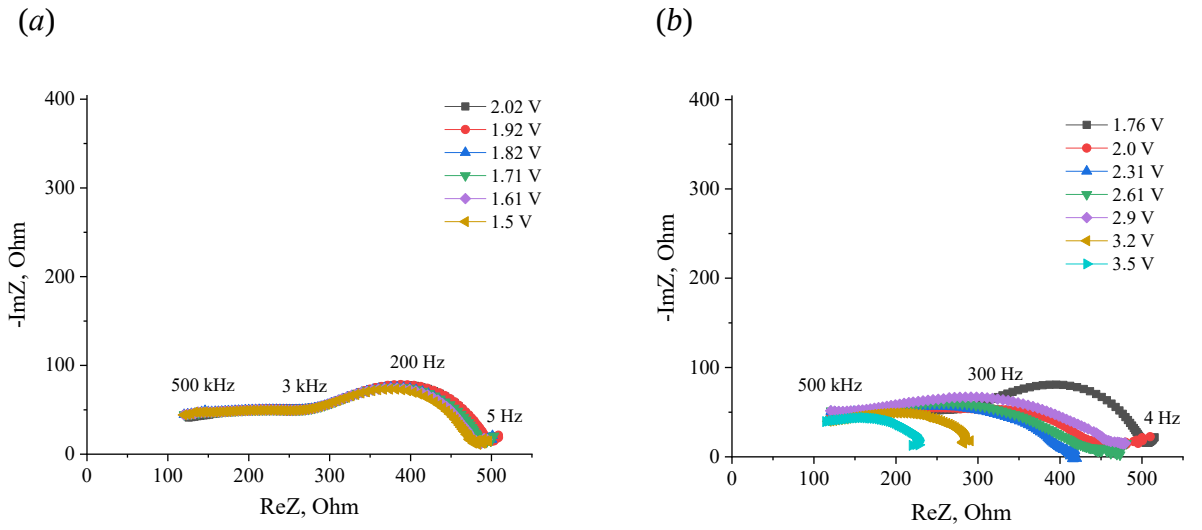
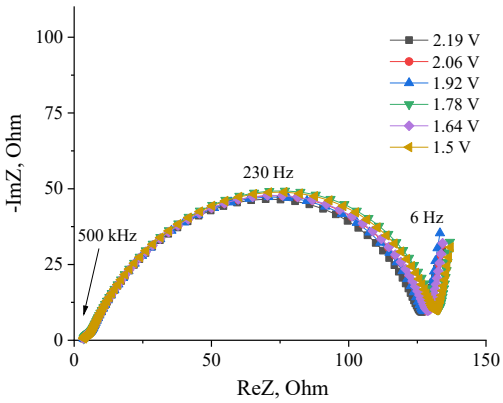
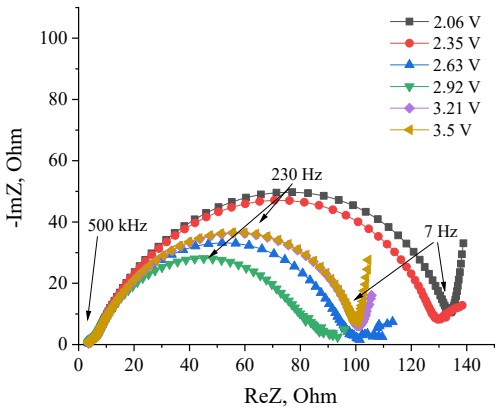


Figure S2 Nyquist plots of Li/LE/PI cells during (*a*) lithiation and (*b*) delithiation.

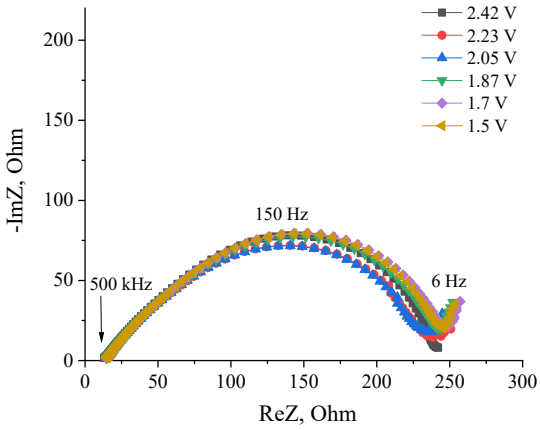
(*a*)


2.19 V
2.06 V
1.92 V
1.78 V
1.64 V
1.5 V
230 Hz
500 kHz
6 Hz
-ImZ, Ohm
ReZ, Ohm

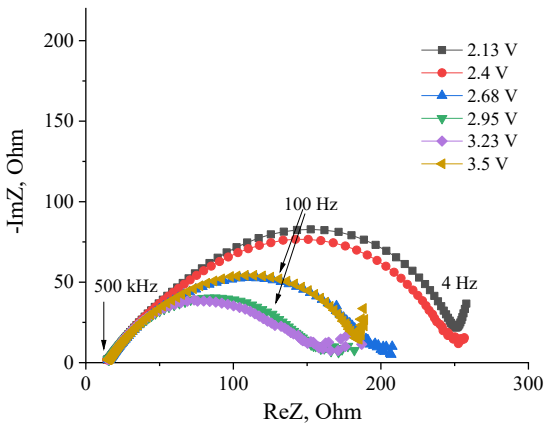
(*b*)


2.06 V
2.35 V
2.63 V
2.92 V
3.21 V
3.5 V
230 Hz
500 kHz
7 Hz
-ImZ, Ohm
ReZ, Ohm

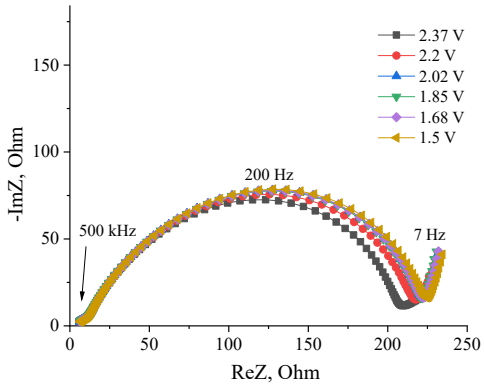
(*c*)


2.42 V
2.23 V
2.05 V
1.87 V
1.7 V
1.5 V
150 Hz
500 kHz
6 Hz
-ImZ, Ohm
ReZ, Ohm

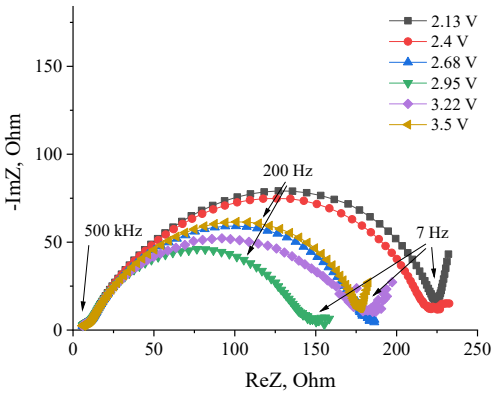
(*d*)

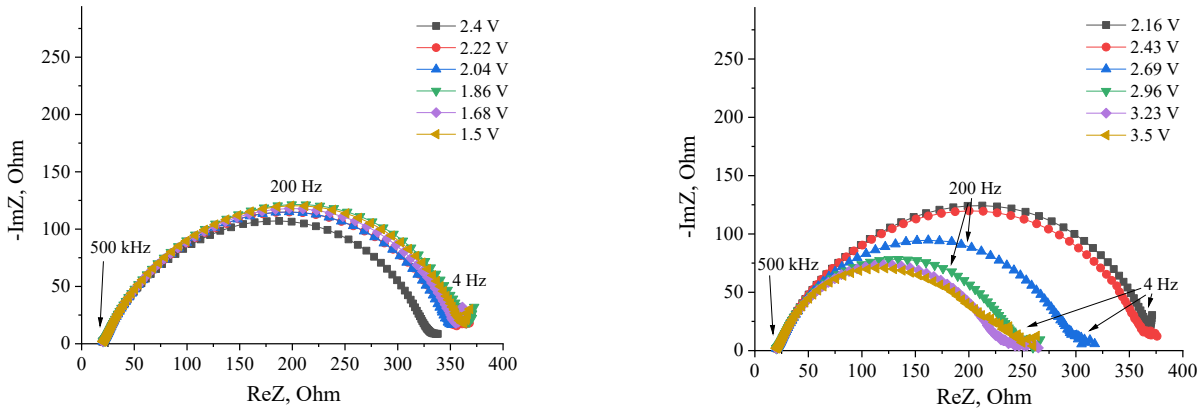

2.13 V
2.4 V
2.68 V
2.95 V
3.23 V
3.5 V
100 Hz
500 kHz
4 Hz
-ImZ, Ohm
ReZ, Ohm

(*e*)


2.37 V
2.2 V
2.02 V
1.85 V
1.68 V
1.5 V
200 Hz
500 kHz
7 Hz
-ImZ, Ohm
ReZ, Ohm

(*f*)


2.13 V
2.4 V
2.68 V
2.95 V
3.22 V
3.5 V
200 Hz
500 kHz
7 Hz
-ImZ, Ohm
ReZ, Ohm



(*g*) (*h*)

Figure S3 Nyquist plots Li//PI cells with electrolytes: (*a*)–(*b*) LE + 5 % Pol-1, (*c*)–(*d*) LE + 10 % Pol-1; (*e*)–(*f*) LE + 5 % Pol-2, (*g*)–(*h*) LE + 10 % Pol-2 during (*a*),(*c*),(*i*),(*g*) lithiation and (*b*),(*d*),(*f*),(*h*) delithiation.

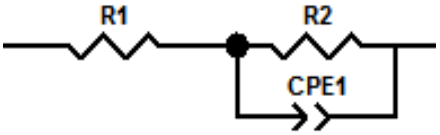


Figure S4 Equivalent circuit of Li//PI cell, where *R*1 – electrolyte resistance, *R*2 – charge-transfer resistance at the lithium/electrode interface, CPE – constant phase element.

Table S2 Calculation of the parameters of the equivalent circuit of the Li/PI cell.

Electrolyte	*R*1/ Ohm cm^2	*R*2/ Ohm cm^2	CPE-T/ F cm^{-2}	CPE-P	R1/ Ohm cm^2	R2/ Ohm cm^2	CPE-T, F cm^{-2}	CPE-P
	Lithiation (1.92V)				Delithiation (1.76 V)			
LE	**250**	258	4.2×10^{-5}	0.69	**250**	266	3.8×10^{-5}	0.69
	Lithiation (2.06V)				Delithiation (2.68V)			
+ 5 % Pol-1	5.3	131	5.2×10^{-5}	0.77	5.4	94	4.6×10^{-5}	0.77
+ 10 % Pol-1	15.4	239	12×10^{-5}	0.64	17.1	184	10×10^{-5}	0.66
+ 5 % Pol-2	9.6	228	4.0×10^{-5}	0.73	9.4	176	3.6×10^{-5}	0.74
+ 10 % Pol-2	20.6	343	2.8×10^{-5}	0.74	21.4	278	2.2×10^{-5}	0.76



Pristine lithium | Lithium after cycling in liquid electrolyte | Lithium after cycling in Pol-containing electrolyte

Figure S5 Optical images of the lithium anode surface.

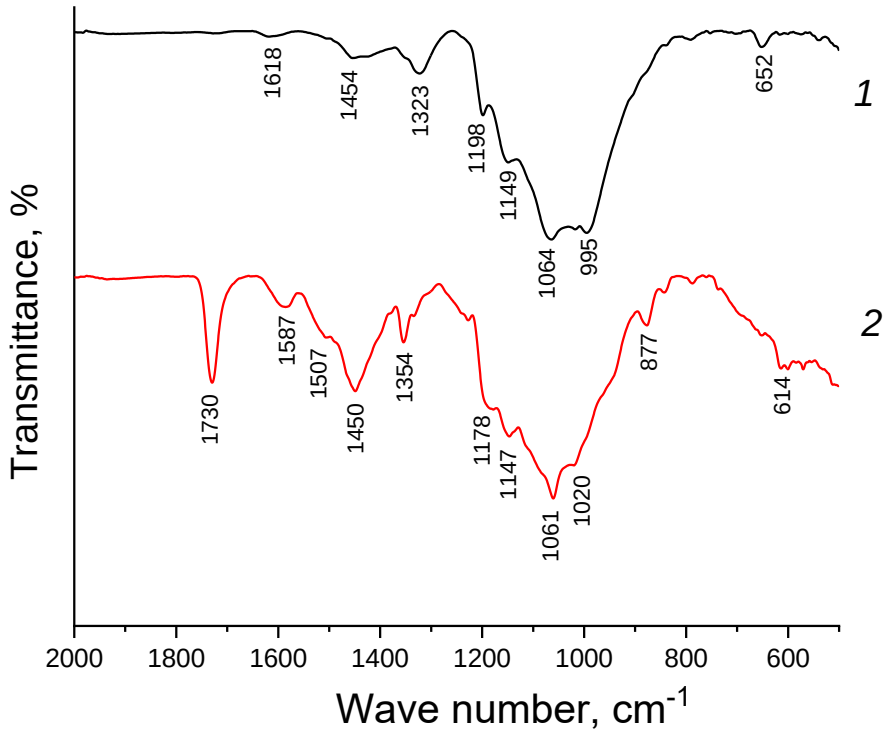
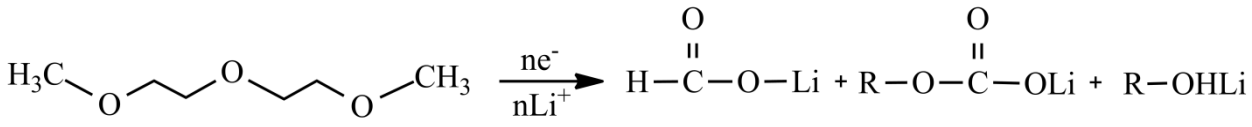


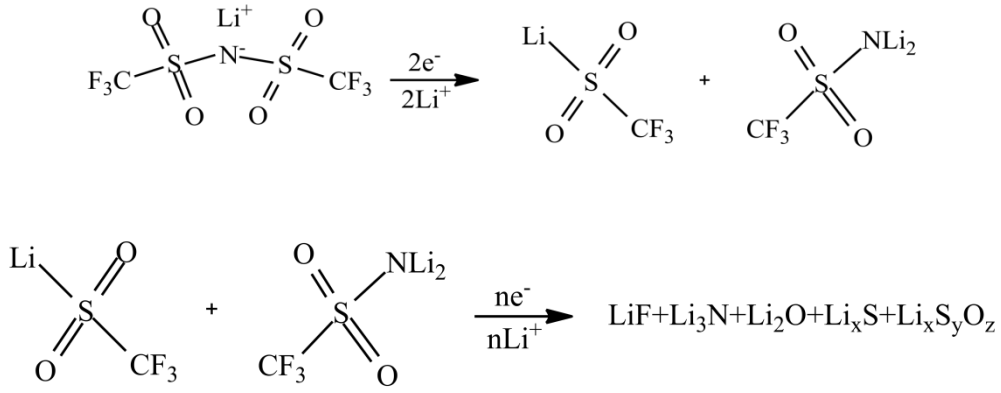
Figure S6 FTIR spectra: (*1*) lithium surface after testing in a cell with a liquid electrolyte; (*2*) lithium surface after testing in a cell with an oligomer-containing electrolyte.

Table S3 Assignment of characteristic peaks of SEI.

Peaks, cm^{-1}	Assignment	Ref.
1730	–C═O carbonyl group of polymer	[S1]
1450, 1454	$–CH_2–$stretching	[S2]
1061, 1323,1354	O═S═O stretching	[S3]
1185, 1228	C–F stretching	[S4]
~700	Li─N stretching	[S5]
600, 616	S–N–S stretching	[S6]



Scheme S1 The diglyme decomposition reaction.



Scheme S2 The LiTFSI decomposition reactions.

References

S1 A. V. Yudina, G. R. Baymuratova, G. Z. Tulibaeva, A. L. Litvinov, A. F. Shestakov and O. V. Yarmolenko, *Russ. Chem. Bulletin*, 2020, **69**, 1455; https://doi.org/10.1007/s11172-020-2923-3.

S2 E. Pretsch, P. Biihlmann and C. Affolter, *Structure Determination of Organic Compounds*, Springer-Verlag, Berlin Heidelberg, 2000; https://doi.org/10.1007/978-3-662-04201-4.

S3 W. Kam, C.-W. Liew, J. Y. Lim and S. Ramesh, *Ionics*, 2014, **20**, 665; https://doi.org/10.1007/s11581-013-1012-0.

S4 L. Wu, J. Hu, S. Chen, S. Yang, X. Liu, L. Foord, J. S. Foord, P. Pobedinskas, K. Haenen, H. Hou and J. Yang, *Electrochim. Acta*, *2023*, **466**, 142973; https://doi.org/10.1016/j.electacta.2023.142973.

S5 D. Aurbach, E. Pollak, R. Elazari, G. Salitra, C. S. Kelley and J. Affinito, *J. Electrochem. Society*, 2009, **156**, A694; https://doi.org/10.1149/1.3148721.

S6 Q. Rey, P. Johansson, J. Lindgren, J. C. Lassègues, J. Grondin and L. Servant, *J. Phys. Chem. A*, 1998, **102**, 3249; https://doi.org/10.1021/jp980375v.